DOI: 10.1002/chem.200700420

# Photoreactivity and Photopolymerization of Silicon-Bridged [1]Ferrocenophanes in the Presence of Terpyridine Initiators: Unprecedented Cleavage of Both Iron–Cyclopentadienyl Bonds in the Presence of Chlorosilanes

**Wing Yan Chan,[b] Alan J. Lough,[b] and Ian Manners*[a, b]**

**Abstract:** The photopolymerisation of sila[1]ferrocenophane [Fe(η-$C_5H_4$)$_2$-$SiMe_2$] (**3**) with 4,4′,4″-tri-*tert*-butyl-2,2′:6′,2″-terpyridine (*t*$Bu_3$terpy) as initiator has been explored. High-molecular-weight polyferrocenylsilane (PFS) [{Fe(η-$C_5H_4$)$_2$$SiMe_2$}$_n$] (**5**) was formed in high yield when a stoichiometric amount of *t*$Bu_3$terpy was used at 5 °C. Photopolymerisation of ferrocenophane **3** at higher temperatures gave PFS **5** in lower yield and with a reduced molecular weight as a result of a slower propagation rate. Remarkably, when $Me_3SiCl$ was added as a capping agent before photopolymerisation, subsequent photolysis of the reaction mixture resulted in the unprecedented cleavage of both iron–Cp bonds in ferrocenophane **3**: iron(II) complex [Fe(*t*$Bu_3$terpy)$_2$$Cl_2$] (**7**$_{Cl}$) was formed and the silane fragment ($C_5H_4SiMe_3$)$_2$$SiMe_2$ (**8**) was released. The iron–Cp bond cleavage reaction also proceeded in ambient light, although longer reaction times were required. In addition, the unexpected cleavage chemistry in the presence of $Me_3SiCl$ was found to be applicable to other photoactive ferrocenes such as benzoylferrocene. For benzoylferrocene and ferrocenophane **3**, the presence of metal-to-ligand charge transfer (MLCT) character in their low-energy transitions in the visible region probably facilitates photolytic iron–Cp bond cleavage, but this reactivity is suppressed when the strength of the iron–Cp bond is increased by the presence of electron-donating substituents on the cyclopentadienyl rings.

**Keywords:** chlorosilane · cyclopentadienyl ligands · ferrocenophanes · N ligands · ring-opening polymerization

## Introduction

Molecules that possess ring strain are of great interest, as they participate in a variety of reactions with the accompanying release of strain energy. An excellent example is provided by the silicon-bridged [1]ferrocenophanes (sila[1]-ferrocenophanes) discovered by Osborne and co-workers in 1975.[1–4] These molecules are strained since the bridging silicon atom forces the two cyclopentadienyl rings in ferrocene to tilt towards each other by a dihedral angle of approximately 21°.[5] Indeed, differential scanning calorimetry showed that the strain energy in sila[1]ferrocenophanes is between 70 and 80 kJ mol$^{-1}$.[6] To relieve ring strain, sila[1]-ferrocenophanes readily undergo ring-opening reactions when they are treated with proton sources to give silyl-substituted ferrocenes.[7–9] In addition, sila[1]ferrocenophanes undergo ring-opening polymerisation (ROP) upon exposure to heat, anionic initiators, or transition-metal catalysts.[10] For both of these types of ring-opening reactions, ring strain is relieved through cleavage of the *ipso*-Cp carbon–silicon bond. Ferrocenophanes with a larger bridging atom such as tin have also been synthesised and they possess smaller tilt angles and correspondingly less ring strain.[11] Despite the reduction in strain, these compounds undergo similar ring-opening reactions and the insertion of metal–carbonyl fragments into the *ipso*-Cp carbon–tin bond of a stanna[1]ferrocenophane has been observed.[12]

In contrast to cleavage of the *ipso*-Cp carbon-bridging atom bond, relief of ring strain by breaking the iron–Cp bond in ferrocenophanes has only recently been identified.[13] The first examples involved iron–Cp bond cleavage

[a] Prof. I. Manners
School of Chemistry, University of Bristol
Bristol, England, BS8 1TS (UK)
Fax: (+44) 117-929-0509
E-mail: Ian.Manners@Bristol.ac.uk

[b] W. Y. Chan, Dr. A. J. Lough, Prof. I. Manners
Department of Chemistry, University of Toronto
80 St. George Street, Toronto, Ontario, M5S 3H6 (Canada)

  

in boron- or phosphorus-bridged ferrocenophanes. In 2000, our group and that of Braunschweig reported that boron-bridged ferrocenophanes react with $[Fe_2(CO)_9]$ or $[Co_2(CO)_8]$ and metal–carbonyl fragments are inserted into an iron–Cp bond.[14] Later in 2003, Miyoshi and co-workers showed that phosphorus-bridged ferrocenophanes undergo iron–Cp bond cleavage when irradiated with UV light in the presence of phosphanes and phosphites; one of the Cp ligands dissociates and the incoming phosphane or phosphite coordinates to the iron centre.[15] When the phosphane or phosphite is absent, ROP of the phosphorus-bridged ferrocenophane was observed in THF.[16] To the best of our knowledge, there are only two published examples of iron–Cp bond cleavage in silicon-bridged ferrocenophanes.[17,18] In 2004, our group reported that sila[1]ferrocenophanes undergo ROP when treated with $Na[C_5H_5]$ and UV light (Scheme 1).[17] This reaction proceeds through an iron–Cp

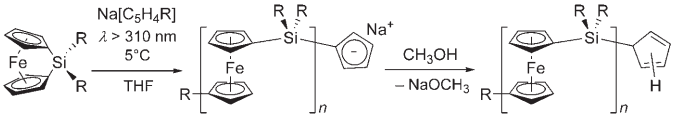


Scheme 1. Photocontrolled ring-opening polymerisation of ferrocenophanes to give polyferrocenylsilanes.

bond cleavage mechanism as the incoming Cp anion displaces one of the Cp ligands in the ferrocenophane. A living polymerisation follows and polyferrocenylsilanes (PFS) with controllable molecular weight and with low polydispersity are obtained. This is possible because each Cp anion generates one polymer chain, initiation is fast and no significant chain transfer or termination steps occur.

In addition to iron–Cp bond cleavage, sila[1]ferrocenophanes have been found to undergo reversible $\eta^5$–$\eta^1$ ring slippage in the presence of phosphanes (Scheme 2).[19] Pho-

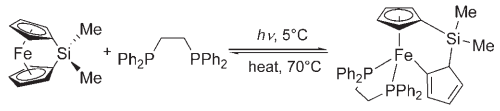


Scheme 2. Reversible haptotropic shift of a Cp ligand in a [1]ferrocenophane.

tolysis of a solution containing a [1]ferrocenophane and 1,2-bis(diphenylphosphino)ethane resulted in slippage of a Cp ring from an $\eta^5$ to an $\eta^1$ coordination mode; when the ring-slipped product was heated at 70°C, quantitative extrusion of the phosphane occurred and the [1]ferrocenophane was regenerated. Isolation of the ring-slipped product is significant as it suggests the photopolymerisation of ferrocenophanes in donor solvents such as THF may involve a ring-slipped species, with THF solvent molecules occupying the coordination sites vacated by the ring-slipped Cp ring.

The aforementioned interesting and unexpected discoveries concerning the photopolymerisation of sila[1]ferrocenophanes prompted us to perform in depth studies of the photoreactivity of these interesting strained species. In this paper we report on our exploration of non-Cp-based initiators. The ligands chosen for this study were 4,4′,4″-tri-*tert*-butyl-2,2′:6′,2″-terpyridine (**1**, $t$Bu$_3$terpy) and 2,2′:6′,2″-terpyridine (**2**).

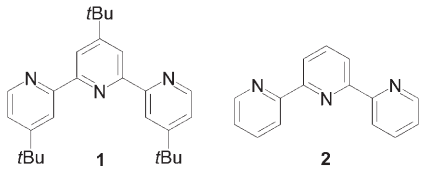

## Results and Discussion

**Attempted photolytic ring-opening of sila[1]ferrocenophane 3 using terpyridine 1—formation of polyferrocenylsilane 5**: To study the reactivity of monomer **3** towards terpyridine initiator **1**, we first attempted to stoichiometrically ring-open the monomer to form **4a**[20] (Scheme 3). A solution containing equimolar amounts of monomer **3** and terpyridine **1** in THF was photolysed with a mercury lamp for 1 h at 5°C. The colour of the solution changed from red to brownish green, and precipitation of the reaction mixture into $Et_2O$ gave a yellow powder in 82% yield. The $^1$H NMR spectrum of the powder showed peaks consistent with PFS **5**,[21] and GPC analysis of the polymer gave $M_n = 40100$ and PDI = 1.55.

The formation of polymer in this stoichiometric reaction suggests that chain propagation is much faster than monomer initiation. Thus when monomer **3** is ring-opened by terpyridine **1**, the subsequent product presumably immediately reacts to rapidly ring-open more monomer units to form PFS **5**. When the above reaction was performed at 20°C, PFS **5** was formed in 76% yield with a bimodal molecular weight distribution ($M_n = 59000$, PDI = 1.51, 71% of all polymer; $M_n = 7600$, PDI = 1.32, 29% of all polymer). When

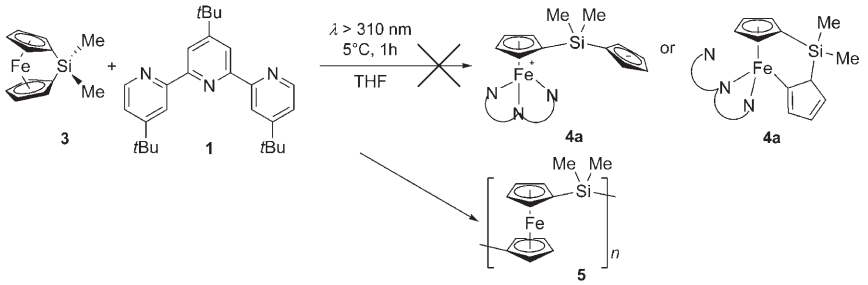


Scheme 3. Attempted photolytic ring-opening of monomer **3** in the presence of terpyridine **1**.

  

we carried out the reaction at an even higher temperature (35 °C), the yield of PFS **5** dropped still further to 29 % and a lower molecular weight was observed ($M_n$ = 20 600, PDI = 1.79).

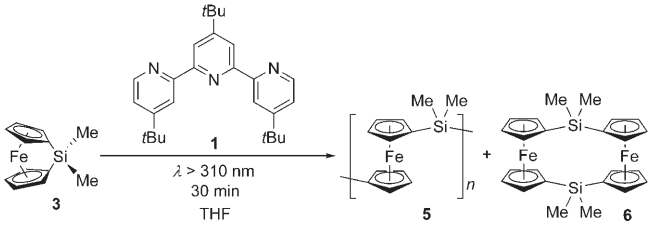


Scheme 4. Formation of PFS **5** and cyclic dimer **6** in the photolysis of monomer **3**.

Table 1. Photopolymerisation of monomer **3** with **1** as initiator at various temperatures.[a]

| | *T* [°C] | Monomer **3** [%] | Polymer **5** [%] | Cyclic dimer **6** [%] |
|---|---|---|---|---|
| 1 | 5 | 1 | 97 | 2 |
| 2 | 20 | 10 | 84 | 6 |
| 3 | 35 | 63 | 27 | 10 |

[a] Analysis by $^1$H NMR spectroscopy in $C_6D_6$ after photolysis for 30 min in THF.

Previous work by our group has revealed that the propagation rate for the photopolymerisation decreases with increasing temperature when Na[$C_5H_5$] was used as initiator.[18,22] To confirm that the propagation rate also decreases with increasing temperature in the terpyridine-initiated photopolymerisation, conversion to polymer was measured by $^1$H NMR spectroscopy after 30 minutes of irradiation at three different temperatures. The results of these experiments are summarised in Scheme 4 and Table 1.

For the reaction at 5 °C, analysis of the reaction mixture by $^1$H NMR spectroscopy showed 97 % conversion to PFS **5**.[23] Conversion to PFS **5** only reached 84 % for the reaction at 20 °C, and 27 % for the reaction at 35 °C. The reduced conversion to polymer at higher temperatures confirmed that propagation rates are slower, resulting in lower molecular weights.[24] Surprisingly, cyclic dimer **6**[25] was also formed in all three cases and was present in an increasingly larger amounts at the higher temperatures. A possible route to cyclic dimer **6** is backbiting of the growing polymer chain.[26] Since propagation is slower at higher temperatures, it is likely that the backbiting reaction becomes more significant at these temperatures, producing a larger amount of **6**.

A plausible mechanism for the photopolymerisation of monomer **3** and the formation of cyclic dimer **6** is shown in Scheme 5. Photolysis of monomer **3** and *t*Bu$_3$terpy should give species **4a**[20] (not observed), which rapidly reacts with additional units of monomer **3** to form a PFS polymer chain (**5a**). The broad molecular-weight distribution (in some cases bimodal) observed for PFS **5** may be explained by the presence of backbiting and macrocondensation reactions. Backbiting occurs when the propagating Cp anion of PFS **5a** attacks the iron centre in the previous repeat unit, releasing *t*Bu$_3$terpy and cyclic dimer **6**. Alternatively, the propagating Cp anion from PFS **5a** could attack the Fe centre at the head of a neighbouring PFS chain in a macrocondensation reaction to give *t*Bu$_3$terpy and an elongated PFS chain (**5b**).

As terpyridine **1** initiated the polymerisation of monomer **3**, we also investigated the possibility of molecular weight control. Three different monomer to initiator ratios were examined and the results are summarised in Table 2.

Unlike the photopolymerisation that utilises Na[$C_5H_5$] as initiator, the use of terpyridine **1** does not allow efficient molecular weight control in the polymerisation of monomer **3**. As the amount of initiator decreased, so did the molecular weight and also the isolated yield of PFS **5**. These results suggest that terpyridine **1** is an inefficient initiator for the photopolymerisation of **3**.

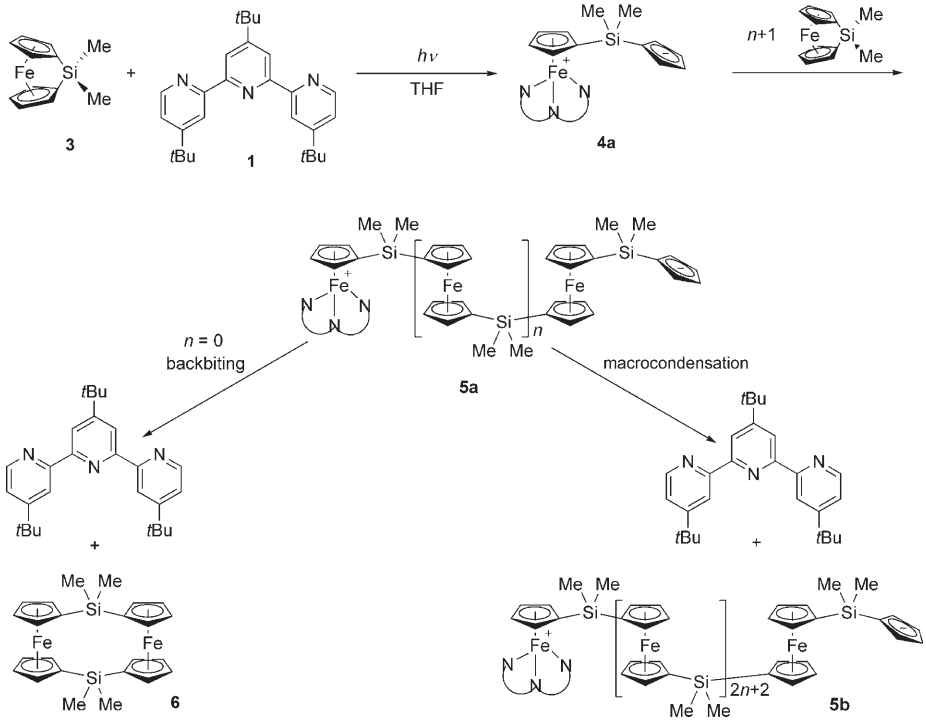


Scheme 5. Possible backbiting and chain transfer reactions in the photopolymerisation of monomer **3** using *t*Bu$_3$terpy as initiator.

Table 2. Photopolymerisation of monomer **3** using terpyridine **1** at 5°C.

| [M]:[I] | $t$ [h] | $M_n$ expected | $M_n$ found[a] | PDI | Isolated yield of **5** [%] |
|---|---|---|---|---|---|
| 25:1 | 2 | 6100 | $1.0\times10^5$ (0.36) | 1.33 | 43 |
| | | | 9300 (0.64) | 1.52 | |
| 50:1 | 2 | 12100 | 61600 (0.48) | 1.28 | 16 |
| | | | 5500 (0.52) | 1.30 | |
| 75:1 | 4 | 18200 | 53800 (0.55) | 1.33 | 5 |
| | | | 5300 (0.45) | 1.22 | |

[a] All molecular weight distributions were bimodal, and the number in parentheses indicate the relative amounts of each fraction.

**Photolysis of sila[1]ferrocenophane 3 in the presence of terpyridine and trimethylsilyl chloride—unexpected formation of bis(terpyridine)iron complex $7_{Cl}$**: Since it was not possible to prepare compound **4a**[20] from equimolar amounts of monomer **3** and terpyridine **1**, we decided to add $Me_3SiCl$ to the mixture before UV irradiation to immediately cap this species during the photolysis and allow the isolation of derivative **4b**[20] (Scheme 6). However, surprisingly copious amounts of a purple precipitate were formed after this solution was photolysed for 1 h at 5°C. The purple colour is diagnostic for a $[Fe(terpyridine)_2]^{2+}$ ion. Purple solid $\mathbf{7}_{Cl}$ was isolated by filtration in the glovebox and dried under vacuum. Analysis of the orange filtrate by $^1H$ NMR spectroscopy showed resonances for unreacted monomer **3** (ca. two equivalents with respect to unreacted **1**), terpyridine **1**, silane **8**, and PFS **5** (ca. one equivalent with respect to unreacted **1**). We also characterised silane **8** using HRMS and GC-MS. Analysis of the orange filtrate by HRMS showed a molecular ion at $m/z = 332.181802$, which corresponds to the composition $C_{18}H_{32}Si_3$. Separation of the different compounds in the filtrate was accomplished by means of GC-MS, and the major component had a $m/z$ ratio of 332. Analysis of its major fragments in the mass spectrum confirmed the structure of silane **8** as $[(C_5H_4SiMe_3)_2SiMe_2]$ (see Experimental Section).

Purple solid $\mathbf{7}_{Cl}$ was identified by NMR spectroscopy and mass spectrometry. The $^1H$ NMR spectrum of $\mathbf{7}_{Cl}$ corresponds to that of a coordinated terpyridine ligand, as protons *ortho* to the nitrogen atoms, H6 and H6″, showed the characteristic upfield shift (from $\delta = 8.77$ ppm to $\delta = 6.88$ ppm) after metal coordination.[27] ESI-MS analysis of $\mathbf{7}_{Cl}$ showed a doubly charged molecular ion peak at $m/z = 429.25$, which corresponds to the composition $[C_{54}H_{70}N_6Fe]^{2+}$. From these data, we deduced the structure of $\mathbf{7}_{Cl}$ to be $[Fe(t\mathrm{Bu}_3\mathrm{terpy})_2]Cl_2$.[28]

We attempted to confirm the molecular structure of $\mathbf{7}_{Cl}$ by X-ray crystallography, but we were unable to grow satisfactory crystals despite numerous attempts. When the $Cl^-$ ions in $\mathbf{7}_{Cl}$ were exchanged with $PF_6^-$ to give $\mathbf{7}_{PF_6}$,[29] we succeeded in obtaining X-ray quality crystals of $\mathbf{7}_{PF_6}$ by diffusion of $Et_2O$ vapour into a solution of $\mathbf{7}_{PF_6}$ in THF. Figure 1 shows the molecular structure of $\mathbf{7}_{PF_6}$ and Table 3 contains selected geometric parameters for this compound.

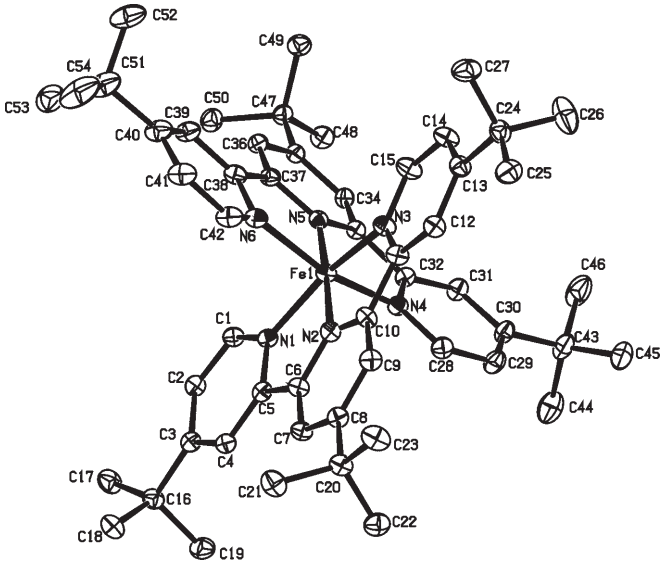


Figure 1. Molecular structure of $\mathbf{7}_{PF_6}$ (thermal ellipsoids at 30% probability). Hydrogen atoms have been removed for clarity and the $PF_6$ anions are not shown.

The molecular structure of $\mathbf{7}_{PF_6}$ confirmed the anticipated atomic arrangement. As in other $[Fe(terpyridine)_2]^{2+}$ ions,[30] the terpyridine ligands in $\mathbf{7}_{PF_6}$ are bound in a meridional fashion. The bite angles of the two terpyridine ligands are 161.87(10)° (N1-Fe1-N3) and 161.20(10)° (N4-Fe1-N6) and the large deviation from linearity suggests the iron atom is in a distorted octahedral environment. Indeed, the cation exhibits tetragonal compression and two of the six Fe–N bonds ($d$(Fe1–N2) = 1.879(2) Å, $d$(Fe1–N5) = 1.878(2) Å) are shorter than the remaining four Fe–N bonds (av 1.968 Å). As a result, the pyridine rings containing N2 and N5 can be con-

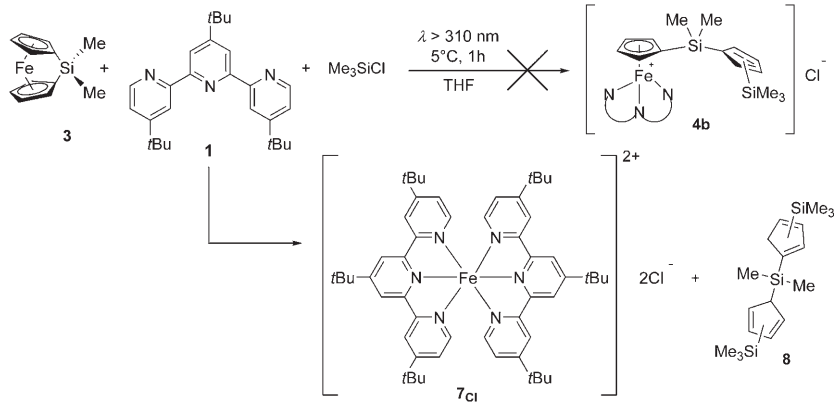


Scheme 6. Attempted photolytic ring-opening of monomer **3** in the presence of terpyridine **1** and trimethylsilyl chloride, unexpected formation of iron bis(terpyridine) complex $\mathbf{7}_{Cl}$.

Table 3. Selected bond lengths [Å] and angles [°] for $\mathbf{7}_{PF_6}$.

| | | | |
|---|---|---|---|
| Fe1–N1 | 1.961(2) | N1-Fe1-N3 | 161.87(10) |
| Fe1–N2 | 1.879(2) | N4-Fe1-N6 | 161.20(10) |
| Fe1–N3 | 1.964(3) | N1-Fe1-N4 | 92.76(10) |
| Fe1–N4 | 1.970(2) | N3-Fe1-N4 | 91.11(10) |
| Fe1–N5 | 1.878(2) | N3-Fe1-N6 | 88.87(10) |
| Fe1–N6 | 1.978(2) | N6-Fe1-N1 | 93.08(10) |
| N1–C1 | 1.341(4) | C1-N1-C5 | 116.2(2) |
| N1–C5 | 1.368(4) | C6-N2-C10 | 120.6(2) |
| N2–C6 | 1.353(4) | C11-N3-C15 | 118.0(3) |
| N2–C10 | 1.350(4) | C28-N4-C32 | 117.6(2) |
| N3–C11 | 1.365(4) | C33-N5-C37 | 120.1(2) |
| N3–C15 | 1.336(4) | C38-N6-C42 | 117.8(2) |
| N4–C28 | 1.345(3) | | |
| N4–C32 | 1.367(4) | | |
| N5–C33 | 1.350(3) | | |
| N5–C37 | 1.358(3) | | |
| N6–C38 | 1.365(4) | | |
| N6–C42 | 1.342(4) | | |

sidered as axial ligands, and the pyridine rings containing N1, N3, N4 and N6 equatorial ligands. The two types of pyridine rings can also be differentiated by inspecting the angle around the nitrogen atom: the average C-N-C angle for axial pyridine rings is 120.4°, while the corresponding angle for equatorial pyridine rings is 117.4°. These structural characteristics are similar to those of the parent $[Fe(terpyridine)_2]^{2+}$ ion without *tert*-butyl groups.[30] There are no close contacts between the cation and anions in $\mathbf{7}_{PF_6}$.

A possible route to $\mathbf{7}_{Cl}$ and **8** is illustrated in Scheme 7. Photolysis of monomer **3** and $t$Bu$_3$terpy should generate ring-opened monomer **4a**[20] (not observed), and the pendent Cp ligand presumably reacts immediately with one equivalent of $Me_3SiCl$ to give compound **4b** (not observed). Because the pendent Cp ligand is capped, ring-opening polymerisation is suppressed and ring-opened monomer **4b** reacts with another molecule of $t$Bu$_3$terpy to form $[Fe(t\text{-}Bu_3terpy)_2]^{2+}$, releasing the bound Cp ligand. Finally, the Cp anion reacts with another equivalent of $Me_3SiCl$, capping the remaining Cp ring to give silane **8**.

After identifying the products formed in this ring-opening reaction, we studied the factors that might affect the yield of $\mathbf{7}_{Cl}$. We varied the photolysis time, the chlorosilane, the terpyridine, and the light source. Table 4 summarises the results of these experiments.

Table 4. Photolytic ring-opening of **3** at 5 °C.

| | **3** [equiv] | Terpyridine **1** [equiv] | $Me_3SiCl$ [equiv] | $t$ [h] | Yield of $\mathbf{7}_{Cl}$[a] [±5%] |
|---|---|---|---|---|---|
| 1 | 1.0 | 1.0 | 1.5 | 1 | 91 |
| 2 | 1.0 | 1.0 | 1.5 | 2 | 85 |
| 3 | 1.0 | 1.0 | 1.5 | 48[b] | 44 |
| 4 | 1.0 | 1.0 | 1.5 | 72[c] | <1 |
| 5 | 1.0 | 1.0 | 1.5[d] | 2 | 59 |
| 6 | 1.0 | 1.0[e] | 1.5 | 1 | 39[f] |

[a] Isolated yield based on **1**. Errors ca. ±5% [b] Reaction was kept at 25 °C and only exposed to ambient light, not UV light. [c] No irradiation was performed and the reaction vessel was kept in the dark at 25 °C and wrapped in Al foil to exclude all ambient light. [d] $Ph_3SiCl$ was used. [e] 2,2′:6′,2″-Terpyridine (**2**) was used. [f] The analogue of $\mathbf{7}_{Cl}$ (without *tert*-butyl groups) was formed.

High yields of $\mathbf{7}_{Cl}$ (up to 91%) were obtained with either 1 h or 2 h of photolysis at 5 °C (entry 1 and 2, Table 4). Remarkably, the reaction also proceeded in ambient light (without UV irradiation), giving a 44% yield of $\mathbf{7}_{Cl}$ after 48 h (entry 3). However, when the reaction vessel was kept in the dark and aluminium foil was used to exclude all light, only negligible quantities of $\mathbf{7}_{Cl}$ were formed (entry 4). This reaction is also applicable to other silyl chlorides, but replacement of $Me_3SiCl$ with $Ph_3SiCl$ resulted in a reduced yield of $\mathbf{7}_{Cl}$ (entry 2 vs. entry 5). When 2,2′:6′,2″-terpyridine (**2**) was used, the product yield decreased to 39% (entry 6).

**Photolysis of other ferrocenophanes and ferrocenes in the presence of $t$Bu$_3$terpy and $Me_3SiCl$**: To establish the scope of this photoinduced iron–Cp bond cleavage reaction, we subjected a variety of ferrocenophanes and ferrocenes to the optimised reaction conditions (entry 1 in Table 4). The results of these experiments are shown in Table 5.

Of the three unstrained ferrocenes tested in this reaction, no reaction was observed for ferrocene (entry 2) or 1,1′-di-

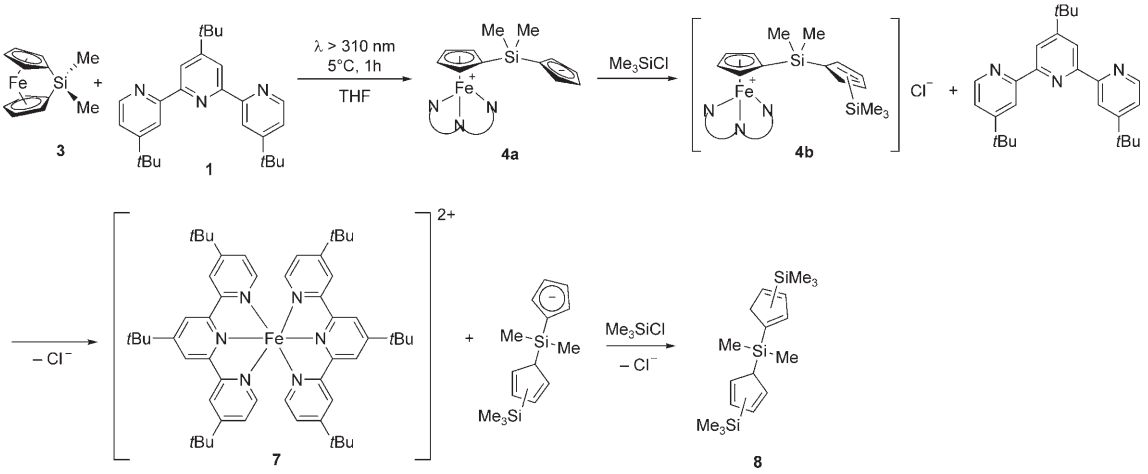


Scheme 7. Possible route for the formation of **7** and **8**.

  

Table 5. Photolytic Fe–Cp bond cleavage in ferrocenes and ferrocenophanes.[a]

| | Compound | $\alpha$ [°] | Isolated yield of $\mathbf{7}_{Cl}$ [%] |
|---|---|---|---|
| 1 | $[Fe(\eta\text{-}C_5H_4)_2SiMe_2]$ (**3**) | 20.8[41] | 91 |
| 2 | $[Fe(\eta\text{-}C_5H_5)_2]$ | 0 | 0 |
| 3 | $[Fe(\eta\text{-}C_5H_4Me)_2]$ | 2.4[42] | 0 |
| 4 | $[Fe(\eta\text{-}C_5H_5)\{\eta\text{-}C_5H_4C(O)Ph\}]$ | 0 | 34 |
| 5 | $[Fe(\eta\text{-}C_5H_4)_2CH_2CH_2]$ | 21.6[43] | 2 |
| 6 | $[Fe(\eta\text{-}C_5H_4)_2SiMe_2SiMe_2]$ | 4.3[44] | 0 |
| 7 | $[Fe(\eta\text{-}C_5H_3t\text{Bu})_2SiPh_2]$ | 18.8[35] | 6 |

[a] The reaction conditions used are identical to that of entry 1 in Table 4 (1 equiv $t$Bu$_3$terpy, 1.5 equiv $Me_3SiCl$, 5 °C, 1 h irradiation).

methylferrocene (entry 3) after 1 h of photolysis. In contrast, benzoylferrocene produced $\mathbf{7}_{Cl}$ in 34% yield (entry 4). This is not surprising since benzoylferrocene is known to undergo photochemical iron–Cp bond cleavage.[31] To study the effect of ring-tilt ($\alpha$) on this reaction, we varied the type and number of bridging element(s) in the ferrocenophane. We tested two different [2]ferrocenophanes that have tilt angles close to that of either a [1]ferrocenophane or ferrocene, respectively. Unlike [1]ferrocenophane **3**, these two [2]ferrocenophanes were essentially unreactive under the reaction conditions. The [2]ferrocenophane with a -$CH_2CH_2$- bridge showed minimal iron–Cp bond cleavage, forming $\mathbf{7}_{Cl}$ in only 2% yield (entry 5), and the [2]ferrocenophane with a -$SiMe_2SiMe_2$- bridge showed no reaction (entry 6). Lastly, we explored the influence of iron–Cp bond strength in this reaction. We used a [1]ferrocenophane containing *tert*-butyl groups on the Cp rings, as the presence of electron-donating groups has been shown to strengthen the iron–Cp bond.[32] The increased iron–Cp bond strength makes the photolytic bond cleavage much more difficult, reducing the yield of $\mathbf{7}_{Cl}$ to 6% (entry 7). The increase in iron–Cp bond strength in the case of electron-donating substituents on the Cp rings also explains the lack of photoreactivity for the [2]ferrocenophane with a -$CH_2CH_2$- bridge (entry 5).

These results suggest the iron–Cp bond cleavage reaction takes place most readily for ferrocene derivatives with appreciable metal-to-ligand charge transfer (MLCT) character in the lowest energy transition.[33] The MLCT character can be introduced by adding an electron-withdrawing benzoyl group in conjugation with the Cp ring (e.g. in benzoylferrocene),[31] or by tilting the Cp rings towards each other (e.g. in [1]ferrocenophane **3**).[34] The iron–Cp bond strength is also an important factor in this reaction: when this bond is strengthened with alkyl substituents on the Cp ring[32,35] (such as in $Fe(\eta\text{-}C_5H_3t\text{Bu})_2SiPh_2$), the tendency for iron–Cp bond cleavage is significantly reduced.

## Conclusion

We have explored the use of $t$Bu$_3$terpy as an alternative initiator to $Na[C_5H_5]$ for the photopolymerisation of sila[1]ferrocenophanes. Compared to $Na[C_5H_5]$, $t$Bu$_3$terpy showed much less molecular weight control and gave lower polymer yields. To understand the polymerisation mechanism, we attempted to trap reactive anionic intermediates using $Me_3SiCl$. Surprisingly, photolysis of a solution containing ferrocenophane **3**, $t$Bu$_3$terpy and $Me_3SiCl$ resulted in dissociation of both Cp ligands in ferrocenophane **3** and very little polymerisation. The bis(terpyridine)iron(II) salt $\mathbf{7}_{Cl}$ was formed and silane fragment **8** derived from the ferrocenophane was released. This reaction occurs readily with UV irradiation, but also proceeds under ambient light, albeit with a slower rate.

The scope of this photolytic iron–Cp bond cleavage reaction was examined by using other ferrocene derivatives. Benzoylferrocene is photoactive and also displayed the same reactivity. However, [2]ferrocenophanes are much more difficult substrates for this reaction and are essentially unreactive. For a [1]ferrocenophane substituted with alkyl groups in the Cp rings, photolytic iron–Cp bond cleavage becomes much more difficult due to the stronger iron–Cp bond. We attribute these reactivity differences to the presence of MLCT character in the low-lying excited states of benzoylferrocene and ferrocenophane **3**, allowing for photochemical cleavage of the iron–Cp bond. Nevertheless, photolytic iron–Cp bond cleavage in a [1]ferrocenophane can be suppressed when the iron–Cp bonds are strengthened by alkyl substitution on the Cp rings. As the photocontrolled ROP of a ferrocenophane also involves the cleavage of an iron–Cp bond,[17,18] we anticipate that the reactivity of a ferrocenophane in the photolytic iron–Cp bond-cleavage reaction described in this work should be a good indicator of whether it will undergo photopolymerisation.

The observation that $t$Bu$_3$terpy is a much less effective initiator than $Na[C_5H_5]$ in the photopolymerisation of sila[1]ferrocenophanes can be explained by considering the electronic and steric demands of these ligands. Since $t$Bu$_3$terpy is a neutral species, it is not expected to bind as strongly to the iron centre of the ferrocenophane as the $Cp^-$ ion. Also, unlike $Cp^-$, which coordinates to the iron atom in a facial geometry, $t$Bu$_3$terpy is more sterically demanding and binds in a meridional fashion. These two factors contribute to the lability of $t$Bu$_3$terpy in the polymer head group of PFS **5a**,[20] allowing it to be displaced by the pendent Cp anion in back-biting and macrocondensation reactions. Our future investigations will focus on six-electron, anionic initiators that bind in a facial geometry (e.g., tris(pyrazolyl)borates) as they should bind more efficiently and function as improved initiators.

## Experimental Section

4,4′,4″-Tri-*tert*-butyl-2,2′:6′,2″-terpyridine, 2,2′:6′,2″-terpyridine, $Ph_3SiCl$, $NH_4PF_6$, ferrocene, 1,1′-dimethylferrocene and benzoylferrocene were purchased from Aldrich and used as received. $Me_3SiCl$ was purchased from Aldrich and distilled before use. Monomer **3** was synthesised according to a literature procedure.[36] Most reactions and manipulations were performed under an atmosphere of pre-purified $N_2$ by using Schlenk techniques or in an inert atmosphere glovebox. Unless specified as ACS grade, solvents were dried by the Grubbs method[37] or standard

  

methods followed by distillation. Photolysis experiments were performed with a Philips HPK 125 mercury lamp with a Pyrex filter, and the reaction vessel was placed in a thermostated water bath to maintain the specified temperature. Compounds **5**, $\mathbf{7}_{Cl}$ and $\mathbf{7}_{PF_6}$ were air-stable and handled in air after workup. $^1$H, $^{13}$C and $^{19}$F NMR spectra were recorded on Varian Unity or Varian Mercury spectrometers. $^1$H resonances were referenced internally to the residual protonated solvent resonances and $^{13}$C resonances were referenced internally to the deuterated solvent resonances. $^{19}$F resonances were referenced externally to $CFCl_3$ and $^{31}$P resonances were referenced externally to $H_3PO_4$. Molecular weights were determined by gel permeation chromatography (GPC) with a Viscotek GPC MAX liquid chromatograph equipped with a Viscotek Triple Detector Array. The triple detector array consists of a deflection refractometer, a four-capillary differential viscometer, and a right-angle laser-light-scattering detector ($\lambda_0 = 670$ nm). Conventional calibration was used and molecular weights were determined relative to polystyrene standards purchased from American Polymer Standards. ACS grade THF was used as the eluent at flow rate of 1.0 mL min$^{-1}$. Electron impact (EI) mass spectra were recorded with a Micromass 70S-250 mass spectrometer in electron impact mode. The calculated isotopic distribution for each ion was in agreement with experimental values. Electrospray ionisation (ESI) mass spectra were recorded with an ABI/Sciex QStar mass spectrometer using MeOH/$H_2O$ containing 0.1% formic acid as mobile phase. GC-MS was performed using a Perkin–Elmer TurboMass mass spectrometer (EI source 70 eV) with an Autosystem XL Gas Chromatograph with programmable pneumatic control. The column was a ZB-5 MS (Phenomenex, USA) with dimensions 30 m × 0.25 mm × 0.25 μm. The GC injector was kept at 300 °C, and the initial column temperature was 40 °C (held for 1 min). A temperature ramp of 25 °C min$^{-1}$ was used until the temperature reached 300 °C, at which it was held constant for 1 min. Helium was used as the carrier gas with a flow rate of 1 mL min$^{-1}$. The MS source temperature was 185 °C and temperature of the transfer line was 225 °C. Elemental analyses were performed using a Perkin–Elmer 2400 C/H/N analyser.

**Reaction of 3 with 4,4′,4″-tri-*tert*-butyl-2,2′:6′,2″-terpyridine (1)**: Compound **3** (51 mg, 0.21 mmol) and terpyridine **1** (86 mg, 0.21 mmol) were dissolved with THF (ca. 2 mL) in a Schlenk tube. The tube was photolysed at 5 °C for 1 h to give a brownish green solution. Precipitation into anhydrous $Et_2O$ (50 mL) gave PFS **5** as a yellow powder that was isolated by filtration. The powder was washed with anhydrous $Et_2O$ until the filtrate was colourless and the solid was dried under high vacuum, yield 42 mg (82%). Analysis of the pale yellow filtrate by $^1$H NMR spectroscopy showed it contained only unreacted terpyridine **1**.

*Data for* ***5***: Its $^1$H NMR spectrum matches the data reported previously:[21] $^1$H NMR (400 MHz, $C_6D_6$, 25 °C): $\delta = 4.28$, 4.11 (brs, 8H; Cp), 0.55 ppm (s, 6H; Me); GPC (conventional calibration) $M_n = 40\,100$, $M_w = 62\,100$, PDI = 1.55.

When this reaction was repeated at higher temperatures, PFS **5** was still formed but with a lower molecular weight and a broader molecular-weight distribution. $^1$H NMR analysis of these filtrates showed unreacted terpyridine **1**, monomer **3** and cyclic dimer **6**. Reaction at 20 °C: 76% yield of PFS **5**, $M_n = 59\,000$, PDI = 1.51, 71% of all polymer; $M_n = 7600$, PDI = 1.32, 29% of all polymer. Reaction at 35 °C: 29% yield of PFS **5**, $M_n = 20\,600$, PDI = 1.79.

For the conversion measurements, the photolysis was stopped after 30 min at each temperature (5 °C, 20 °C, 35 °C) and the solvent was removed in vacuo. Conversion was calculated by comparing the integrations of the resonances for monomer **3**, PFS **5**, and cyclic dimer **6**. The reported conversion is the average of values calculated from Cp and methyl resonances.

**Attempts at molecular weight control in the polymerisation of 3 with 4,4′,4″-tri-*tert*-butyl-2,2′:6′,2″-terpyridine (1), a typical example**: Compound **3** (100 mg, 0.41 mmol) was dissolved in THF (1.35 mL) in a Schlenk tube and a THF solution of terpyridine **1** (0.66 mL of 0.025 M, 0.016 mmol) was added. The total volume of solvent was kept at 2 mL. After 2 h of photolysis at 5 °C, the brown solution was precipitated into rapidly stirred ACS grade hexanes (100 mL). A light brown precipitate was formed and was collected by filtration and dried under high vacuum, yield 43 mg (43%). Its $^1$H NMR spectrum was identical to that of PFS **5**.

**Reaction of 3 with 4,4′,4″-tri-*tert*-butyl-2,2′:6′,2″-terpyridine (1) in the presence of $Me_3SiCl$, a typical example**: Compound **3** (50 mg, 0.21 mmol) and terpyridine **1** (83 mg, 0.21 mmol) were dissolved with THF (ca. 2 mL) in a Schlenk tube. $Me_3SiCl$ (0.04 mL, 0.32 mmol) was added and the solution was photolysed at 5 °C for 1 h. A purple precipitate was formed. A small amount of hexanes was added to ensure complete precipitation of the solid, which was isolated by filtration in the glovebox. The solid was washed with more hexanes and dried under high vacuum to give $\mathbf{7}_{Cl}$, yield 89 mg (91%). The orange filtrate was pumped to dryness to give an orange-red oily solid. $^1$H NMR analysis of the oil showed it contained unreacted **3**, terpyridine **1**, silane **8** and some PFS **5**.

*Data for* $\mathbf{7}_{Cl}$: $^1$H NMR (400 MHz, $CD_3CN$, 25 °C): $\delta = 9.06$ (s, 4H; 3′ and 5′), 8.63 (d, $^4J$(H,H) = 2 Hz, 4H; 3 and 3″), 7.04 (dd, $^3J$(H,H) = 6 Hz, $^4J$(H,H) = 1.5 Hz, 4H; 5 and 5″), 6.88 (d, $^3J$(H,H) = 6 Hz, 4H; 6 and 6″), 1.82 (brs, 18H; *t*Bu at C4′), 1.27 ppm (brs, 36H; *t*Bu at C4 and C4″); $^{13}$C{$^1$H} NMR (125.7 MHz, $CD_3CN$, 25 °C): $\delta = 164.5$, 164.3, 160.9, 159.0, 153.1, 125.1, 122.44, 122.41 (aromatic), 37.6 ($C(CH_3)_3$), 36.2 ($C(CH_3)_3$), 31.3 ($C(CH_3)_3$), 30.5 ppm ($C(CH_3)_3$); ESI-MS (positive mode, MeOH/$H_2O$ eluent): *m*/*z* (%): 429.2 (100) $[M]^{2+}$; elemental composition from ESI-MS: *m*/*z* calcd: 429.2500; found: 429.2487, corresponds to $[C_{54}H_{70}N_6Fe]^{2+}$; elemental analysis calcd (%) for $C_{54}H_{70}N_6FeCl_2$: C 69.75, H 7.59, N 9.04; found: C 66.86, H 7.91, N 8.77. Although the elemental analysis of $\mathbf{7}_{Cl}$ was performed seven times using samples from different batches, satisfactory analytical data have not yet been obtained, most probably due to its incomplete combustion.

The identity of silane **8** was established by MS and GC-MS. Before concentration of the above orange filtrate, its analysis by MS showed a molecular ion peak at *m*/*z* 332 (22%) and other fragments at *m*/*z* 195 (100%) $[M-SiMe_3-C_5H_4]^+$ and 73 (49%) $[SiMe_3]^+$. HRMS of the same sample (EI, 70 eV): *m*/*z* calcd for $C_{18}H_{32}Si_3$: 332.181186; found: 332.181802, fit 1.9 ppm. The orange filtrate was then diluted for analysis by GC-MS. The major component that eluted at 9.5 min showed a molecular ion at *m*/*z* 332. Major peaks: *m*/*z* (%): 332 (1) $[M]^+$, 259 (1) $[M-SiMe_3]^+$, 195 (100) $[M-SiMe_3-C_5H_4]^+$, 122 (27) $[M-2SiMe_3-C_5H_4]^+$, 73 (100) $[SiMe_3]^+$.

**Metathesis reaction of $\mathbf{7}_{Cl}$ with $NH_4PF_6$—synthesis of $\mathbf{7}_{PF_6}$**: Compound $\mathbf{7}_{Cl}$ (86 mg, 0.092 mmol) was dissolved in ACS grade MeOH (1 mL) and a solution of $NH_4PF_6$ (144 mg, 0.88 mmol) in ACS grade MeOH (1 mL) was added dropwise. The mixture was stirred for 10 min and a dark purple precipitate was formed. Distilled $H_2O$ (10 mL) was added and the suspension was filtered through a fritted glass funnel to collect the purple solid. The solid was washed with distilled $H_2O$, ACS grade $Et_2O$ and dried overnight under high vacuum, yield 91 mg (86%). Crystals for a single crystal X-ray diffraction study were obtained by diffusion of $Et_2O$ vapour into a solution of $\mathbf{7}_{PF_6}$ in THF at 25 °C.

*Data for* $\mathbf{7}_{PF_6}$: $^1$H NMR (400 MHz, $CD_3CN$, 25 °C): $\delta = 8.93$ (s, 4H; 3′ and 5′), 8.50 (s, 4H; 3 and 3″), 7.05 (d, $^3J$(H,H) = 6 Hz, 4H; 5 and 5″), 6.87 (d, $^3J$(H,H) = 6 Hz, 4H; 6 and 6″), 1.80 (brs, 18H; *t*Bu at C4′), 1.27 ppm (brs, 36H; *t*Bu at C4 and C4″); $^{19}$F NMR (376 MHz, $CD_3CN$, 25 °C): $\delta = -73.0$ ppm (d, $^1J$(F,P) = 706 Hz, 12F); $^{31}$P NMR (162 MHz, $CD_3CN$, 25 °C): $\delta = -143.5$ ppm (sept, $^1J$(P,F) = 706 Hz, 1P).

**Reaction of 3 with 4,4′,4″-tri-*tert*-butyl-2,2′:6′,2″-terpyridine (1) in the presence of $Ph_3SiCl$**: By using the typical procedure described above, **3** (50 mg, 0.21 mmol), terpyridine **1** (83 mg, 0.21 mmol) and $Ph_3SiCl$ (92 mg, 0.31 mmol) were photolysed in THF (ca. 2 mL) at 5 °C for 2 h. Purple solid $\mathbf{7}_{Cl}$ was formed. In the glovebox, a small amount of hexanes was added to the solution to ensure complete precipitation of $\mathbf{7}_{Cl}$. Filtration through a fritted glass funnel followed by drying under high vacuum gave purple solid $\mathbf{7}_{Cl}$, yield 57 mg (59%). The reddish brown filtrate was pumped to dryness to give a red orange solid, and analysis by $^1$H NMR spectroscopy showed it contained unreacted **3**, terpyridine **1**, $Ph_3SiCl$ and some PFS **5**.

**Reaction of 3 with 2,2′:6′,2″-terpyridine (2) in the presence of $Me_3SiCl$**: By using the typical procedure described above, compound **3** (50 mg, 0.21 mmol), compound **2** (48 mg, 0.21 mmol) and $Me_3SiCl$ (0.04 mL, 0.32 mmol) were photolysed in THF (ca. 2 mL) at 5 °C for 1 h. A purple

  

solid was formed. In the glovebox, a small amount of hexanes was added to the solution to ensure complete precipitation of the solid. Filtration through a fritted glass funnel followed by drying under high vacuum gave the analogue of purple solid $\mathbf{7}_{Cl}$ without *tert*-butyl groups, yield 24 mg (39%). The orange filtrate was pumped to dryness to give a dark red oil, and analysis by $^1$H NMR spectroscopy showed it contained unreacted **3** and **2**, and silane **8**.

**Reaction of ferrocene with 4,4′,4″-tri-*tert*-butyl-2,2′:6′,2″-terpyridine (1) and $Me_3SiCl$**: By using the typical procedure described above, ferrocene (50 mg, 0.27 mmol), terpyridine **1** (109 mg, 0.27 mmol) and $Me_3SiCl$ (0.04 mL, 0.32 mmol) were photolysed in THF (ca. 2 mL) at 5 °C for 1 h. No colour change of the solution was observed and it was pumped to dryness. Analysis by $^1$H NMR spectroscopy showed unreacted ferrocene and terpyridine **1**.

**Reaction of 1,1′-dimethylferrocene with 4,4′,4″-tri-*tert*-butyl-2,2′:6′,2″-terpyridine (1) and $Me_3SiCl$**: By using the typical procedure described above, 1,1′-dimethylferrocene (50 mg, 0.23 mmol), terpyridine **1** (94 mg, 0.23 mmol) and $Me_3SiCl$ (0.05 mL, 0.39 mmol) were photolysed in THF (ca. 2 mL) at 5 °C for 1 h. The solution turned slightly brown and it was pumped to dryness. Analysis by $^1$H NMR spectroscopy showed unreacted 1,1′-dimethylferrocene and terpyridine **1**.

**Reaction of benzoylferrocene with 4,4′,4″-tri-*tert*-butyl-2,2′:6′,2″-terpyridine (1) and $Me_3SiCl$**: By using the typical procedure described above, benzoylferrocene (50 mg, 0.17 mmol), terpyridine **1** (69 mg, 0.17 mmol) and $Me_3SiCl$ (0.04 mL, 0.32 mmol) were photolysed in THF (ca. 2 mL) at 5 °C for 1 h. A purple precipitate was formed. A small amount of hexanes was added to ensure complete precipitation of the solid, which was isolated by filtration in the glovebox. The solid was washed with more hexanes and dried under high vacuum to give $\mathbf{7}_{Cl}$, yield 27 mg (34%). The orange filtrate was pumped to dryness to give an orange-red solid and $^1$H NMR analysis showed it contained unreacted benzoylferrocene and terpyridine **1**.

**Reaction of $[Fe(\eta\text{-}C_5H_4)_2CH_2CH_2]$ with 4,4′,4″-tri-*tert*-butyl-2,2′:6′,2″-terpyridine (1) and $Me_3SiCl$**: By using the typical procedure described above, $[Fe(\eta\text{-}C_5H_4)_2CH_2CH_2]$ (50 mg, 0.24 mmol), terpyridine **1** (96 mg, 0.24 mmol) and $Me_3SiCl$ (0.05 mL, 0.39 mmol) were photolysed in THF (ca. 2 mL) at 5 °C for 1 h. A very fine purple precipitate was formed. A small amount of hexanes was added to ensure complete precipitation of the solid, which was isolated by filtration in the glovebox. The solid was washed with more hexanes and dried under high vacuum to give $\mathbf{7}_{Cl}$, yield 2 mg (2%). The red filtrate was pumped to dryness to give an orange-red solid and $^1$H NMR analysis showed it contained unreacted $[Fe(\eta\text{-}C_5H_4)_2CH_2CH_2]$ and terpyridine **1**.

**Reaction of $[Fe(\eta\text{-}C_5H_4)_2SiMe_2SiMe_2]$ with 4,4′,4″-tri-*tert*-butyl-2,2′:6′,2″-terpyridine (1) and $Me_3SiCl$**: By using the typical procedure described above, $[Fe(\eta\text{-}C_5H_4)_2SiMe_2SiMe_2]$ (50 mg, 0.17 mmol), terpyridine **1** (69 mg, 0.17 mmol) and $Me_3SiCl$ (0.03 mL, 0.24 mmol) were photolysed in THF (ca. 2 mL) at 5 °C for 1 h. No colour change was observed and the solution was pumped to dryness. Analysis by $^1$H NMR spectroscopy showed unreacted $[Fe(\eta\text{-}C_5H_4)_2SiMe_2SiMe_2]$ and terpyridine **1**.

**Reaction of $[Fe(\eta\text{-}C_5H_3t\text{Bu})_2SiPh_2]$ with 4,4′,4″-tri-*tert*-butyl-2,2′:6′,2″-terpyridine (1) and $Me_3SiCl$**: By using the typical procedure described above, $[Fe(\eta\text{-}C_5H_3t\text{Bu})_2SiPh_2]$ (50 mg, 0.10 mmol), terpyridine **1** (43 mg, 0.11 mmol), and $Me_3SiCl$ (0.02 mL, 0.16 mmol) were photolysed in THF (ca. 2 mL) at 5 °C for 1 h. A very fine purple precipitate was formed. A small amount of hexanes was added to ensure complete precipitation of the solid, which was isolated by filtration in the glovebox. The solid was washed with more hexanes and dried under high vacuum to give $\mathbf{7}_{Cl}$, yield 3 mg (6%). The red filtrate was pumped to dryness to give an orange-red solid and $^1$H NMR analysis showed it contained unreacted $[Fe(\eta\text{-}C_5H_3t\text{Bu})_2SiPh_2]$ and terpyridine **1**.

**X-ray crystallography**: Selected crystal, data collection and refinement parameters for $\mathbf{7}_{PF_6}$ are given in Table 6. Single X-ray diffraction data were collected at 150(2) K on a Nonius Kappa-CCD diffractometer and monochromated $Mo_{K\alpha}$ radiation ($\lambda = 0.71073$ Å). The data were integrated and scaled with the Denzo-SMN package.[38] The SHELXTL/PC package was used to solve and refine the structures.[39] Refinement was by full-matrix least-squares on $F^2$ with all data (negative intensities included). Hydrogen atoms were placed in calculated positions and included in the refinement in riding motion approximations.

Table 6. Selected crystal, data collection and refinement parameters for $\mathbf{7}_{PF_6}$.

| | $\mathbf{7}_{PF_6}$ |
|---|---|
| formula | $C_{58}H_{80}F_{12}FeN_6OP_2$ |
| $M_r$ | 1223.07 |
| crystal system | monoclinic |
| space group | $P2_1/n$ |
| colour | purple |
| $a$ [Å] | 16.0673(6) |
| $b$ [Å] | 18.4561(4) |
| $c$ [Å] | 21.5986(8) |
| $\alpha$ [°] | 90 |
| $\beta$ [°] | 100.4110(13) |
| $\gamma$ [°] | 90 |
| $V$ [Å$^3$] | 6299.4(4) |
| $T$ [K] | 150(2) |
| $Z$ | 4 |
| $\rho_{calc}$a [g cm$^{-3}$] | 1.290 |
| $\mu(Mo_{K\alpha})$ [mm$^{-1}$] | 0.368 |
| $F(000)$ | 2568 |
| crystal size [mm$^3$] | $0.30\times0.26\times0.13$ |
| $\theta$ range [°] | 2.56–27.53 |
| reflns collected | 39945 |
| independent reflns | 13922 ($R_{int} = 0.0701$) |
| abs. correction | semi-empirical from equivalents |
| max/min transmission | 0.957/0.879 |
| parameters refined | 677 |
| GoF on $F^2$ | 0.976 |
| $R1$[a] [$I > 2\sigma(I)$] | 0.0610 |
| $wR2$[b] (all data) | 0.1723 |
| largest diff. peak/hole [e Å$^{-3}$] | 0.550/−0.585 |

[a] $R1 = \Sigma\,||F_o| - |F_c||/\Sigma\,|F_o|$. [b] $wR2 = \{\Sigma[w(F_o^2 - F_c^2)^2]/\Sigma[w(F_o^2)^2]\}^{1/2}$.

During the refinement of $\mathbf{7}_{PF_6}$, areas of electron density were located in difference Fourier maps that were assigned as additional diethyl ether solvent molecules. The peak pattern of electron density suggested that the solvent molecule was highly disordered and attempts to model the disorder were unsuccessful. In the final cycles of refinement, the contribution to electron density corresponding to the disordered diethyl ether molecule was removed from the observed data by use of the SQUEEZE option in PLATON.[40] The resulting data vastly improved the precision of the geometric parameters of the remaining structure. The contribution of an additional diethyl ether has been included in the molecular formula of $\mathbf{7}_{PF_6}$.

CCDC-646229 ($\mathbf{7}_{PF_6}$) contains the supplementary crystallographic data for this paper. These data can be obtained free of charge from The Cambridge Crystallographic Data Centre via www.ccdc.cam.ac.uk/data_request/cif.

## Acknowledgements

W.Y.C. thanks the Natural Sciences and Engineering Research Council of Canada for a Canada Graduate Scholarship and the Walter C. Sumner Foundation for a fellowship. I.M. thanks the European Union for a Marie Curie Chair and the Royal Society for a Wolfson Research Merit Award. We thank David Herbert, Dr. Alexandra Bartole-Scott and Georgeta Masson for providing samples of $[Fe(\eta\text{-}C_5H_4)_2CH_2CH_2]$, $[Fe(\eta\text{-}C_5H_4)_2SiMe_2SiMe_2]$ and $[Fe(\eta\text{-}C_5H_3t\text{Bu})_2SiPh_2]$.

[1] a) A. G. Osborne, R. H. Whiteley, *J. Organomet. Chem.* **1975**, *101*, C27-C28; b) J. K. Pudelski, D. A. Foucher, C. H. Honeyman, A. J.

  

Lough, I. Manners, S. Barlow, D. O'Hare, *Organometallics* **1995**, *14*, 2470–2479.
[2] For examples of recent work by other groups on [1]ferrocenophanes, see: a) J. A. Schachner, C. L. Lund, J. W. Quail, J. Müller, *Organometallics* **2005**, *24*, 785–787; b) H. Braunschweig, F. M. Breitling, E. Gullo, M. Kraft, *J. Organomet. Chem.* **2003**, *680*, 31–42; c) Y. Hatanaka, S. Okada, T. Minami, M. Goto, K. Shimada, *Organometallics* **2005**, *24*, 1053–1055; d) I. Sänger, J. B. Heilmann, M. Bolte, H.-W. Lerner, M. Wagner, *Chem. Commun.* **2006**, 2027–2029; e) B. Wrackmeyer, A. Ayazi, W. Milius, M. Herberhold, *J. Organomet. Chem.* **2003**, *682*, 180–187; f) H. K. Sharma, F. Cervantes-Lee, J. S. Mahmoud, K. H. Pannell, *Organometallics* **1999**, *18*, 399–403; g) A. Bucaille, T. Le Borgne, M. Ephritikhine, J.-C. Daran, *Organometallics* **2000**, *19*, 4912–4914; h) T. Mizuta, M. Onishi, K. Miyoshi, *Organometallics* **2000**, *19*, 5005–5009.
[3] For work on related strained metallorings containing different transition metal and/or π-hydrocarbon ligands see: a) J. M. Nelson, A. J. Lough, I. Manners, *Angew. Chem.* **1994**, *106*, 1019–1021; *Angew. Chem. Int. Ed. Engl.* **1994**, *33*, 989–991; b) H. Braunschweig, M. Homberger, C. Hu, X. Zheng, E. Gullo, G. Clentsmith, M. Lutz, *Organometallics* **2004**, *23*, 1968–1970; c) C. Elschenbroich, F. Paganelli, M. Nowotny, B. Neumüller, O. Burghaus, *Z. Anorg. Allg. Chem.* **2004**, *630*, 1599–1606; d) U. Vogel, A. J. Lough, I. Manners, *Angew. Chem.* **2004**, *116*, 3383–3387; *Angew. Chem. Int. Ed.* **2004**, *43*, 3321–3325; e) M. Tamm, A. Kunst, T. Bannenberg, E. Herdtweck, P. Sirsch, C. J. Elsevier, J. M. Ernsting, *Angew. Chem.* **2004**, *116*, 5646–5650; *Angew. Chem. Int. Ed.* **2004**, *43*, 5530–5534; f) A. Berenbaum, I. Manners, *Dalton Trans.* **2004**, 2057–2058; g) A. Bartole-Scott, H. Braunschweig, T. Kupfer, M. Lutz, I. Manners, T.-l. Nguyen, K. Radacki, F. Seeler, *Chem. Eur. J.* **2006**, *12*, 1266–1273; h) C. L. Lund, J. A. Schachner, J. W. Quail, J. Müller, *Organometallics* **2006**, *25*, 5817–5823.
[4] For other work on strained metallorings, see: a) C. Laporte, C. Böhler, H. Schönberg, H. Grützmacher, *J. Organomet. Chem.* **2002**, *641*, 227–234; b) C. Laporte, T. Büttner, H. Rüegger, J. Geier, H. Schönberg, H. Grützmacher, *Inorg. Chim. Acta* **2004**, *357*, 1931–1947, and references therein; c) L. Luo, N. Zhu, N.-J. Zhu, E. D. Stevens, S. P. Nolan, P. J. Fagan, *Organometallics* **1994**, *13*, 669–675; d) C. Li, M. E. Cucullu, R. A. McIntyre, E. D. Stevens, S. P. Nolan, *Organometallics* **1994**, *13*, 3621–3627.
[5] D. E. Herbert, U. F. J. Mayer, I. Manners, *Angew. Chem.* **2007**, *119*, 5152–5173; *Angew. Chem. Int. Ed.* **2007**, *46*, 5060–5081.
[6] J. K. Pudelski, D. A. Foucher, C. H. Honeyman, P. M. Macdonald, I. Manners, S. Barlow, D. O'Hare, *Macromolecules* **1996**, *29*, 1894–1903.
[7] A. B. Fisher, J. B. Kinney, R. H. Staley, M. S. Wrighton, *J. Am. Chem. Soc.* **1979**, *101*, 6501–6506.
[8] M. J. MacLachlan, M. Ginzburg, J. Zheng, O. Knöll, A. J. Lough, I. Manners, *New J. Chem.* **1998**, *22*, 1409–1415.
[9] M. J. MacLachlan, S. C. Bourke, A. J. Lough, I. Manners, *J. Am. Chem. Soc.* **2000**, *122*, 2126–2127.
[10] I. Manners, *Chem. Commun.* **1999**, 857–865.
[11] For example, the presence of tin in the bridge leads to lower ring tilts, see: a) F. Jäkle, R. Rulkens, G. Zech, D. A. Foucher, A. J. Lough, I. Manners, *Chem. Eur. J.*, **1998**, *4*, 2117–2128; b) R. Rulkens, A. J. Lough, I. Manners, *Angew. Chem.* **1996**, *108*, 1929–1931; *Angew. Chem. Int. Ed. Engl.* **1996**, *35*, 1805–1807; c) see reference 2f).
[12] A. Berenbaum, F. Jäkle, A. J. Lough, I. Manners, *Organometallics* **2002**, *21*, 2359–2361.
[13] Cleavage of the iron–Cp bond was considered as a possible mechanism for thermal ring-opening polymerisation of sila[1]ferrocenophanes, but this possibility was ruled out. See: J. K. Pudelski, I. Manners, *J. Am. Chem. Soc.* **1995**, *117*, 7265–7266.
[14] A. Berenbaum, H. Braunschweig, R. Dirk, U. Englert, J. C. Green, F. Jäkle, A. J. Lough, I. Manners, *J. Am. Chem. Soc.* **2000**, *122*, 5765–5774.
[15] T. Mizuta, Y. Imamura, K. Miyoshi, *J. Am. Chem. Soc.* **2003**, *125*, 2068–2069.
[16] T. Mizuta, M. Onishi, K. Miyoshi, *Organometallics* **2000**, *19*, 5005–5009.
[17] M. Tanabe, I. Manners, *J. Am. Chem. Soc.* **2004**, *126*, 11434–11435.
[18] M. Tanabe, G. W. M. Vandermeulen, W. Y. Chan, P. W. Cyr, L. Vanderark, D. A. Rider, I. Manners, *Nat. Mater.* **2006**, *5*, 467–470.
[19] M. Tanabe, S. C. Bourke, D. E. Herbert, A. J. Lough, I. Manners, *Angew. Chem.* **2005**, *117*, 6036–6040; *Angew. Chem. Int. Ed.* **2005**, *44*, 5886–5890.
[20] We thank a referee for suggesting the possibility of terpyridine **1** acting as a bidentate ligand when coordinated to the iron atom of ferrocenophane **3**, in which the third pyridyl ring is weakly bonded or non-bonded to the metal centre. However, our current studies do not provide any information on the ligation mode of terpyridine ligand **1**. For simplicity, terpyridine **1** is shown as a tridentate ligand in compounds **4a**, **4b**, **5a** and **5b**. For further reading, the interested reader can consult a recent article on piano-stool iron(II) complexes containing pyridine ligands: L. Mercs, G. Labat, A. Neels, A. Ehlers, M. Albrecht *Organometallics* **2006**, *25*, 5648–5656.
[21] D. A. Foucher, R. Ziembinski, B. Z. Tang, P. M. Macdonald, J. Massey, C. R. Jaeger, G. J. Vancso, I. Manners, *Macromolecules* **1993**, *26*, 2878–2884.
[22] In this polymerisation, only photoexcited monomers add to the growing polymer chain. We assume that the photoexcited monomer has a shorter lifetime at higher temperatures; therefore, a lower concentration of the photoexcited monomer is present for photopolymerisation and the propagation rate is slower.
[23] Conversion to polymer was calculated by comparing the integrations of $^1$H NMR signals from monomer **3**, PFS **5**, and cyclic dimer **6**. See Experimental Section for details.
[24] These molecular weights are too high for the identification of polymer end groups by NMR spectroscopy.
[25] D. L. Zechel, D. A. Foucher, J. K. Pudelski, G. P. A. Yap, A. L. Rheingold, I. Manners, *J. Chem. Soc., Dalton Trans.* **1995**, *11*, 1893–1899.
[26] The dimerisation of **3** to form **6** has been ruled out: a solution of **3** in THF was photolysed at 5 °C and $^1$H NMR analysis after 1 h of photolysis showed no reaction.
[27] H. Elsbernd, J. K. Beattie, *J. Inorg. Nucl. Chem.* **1972**, *34*, 771–774.
[28] The presence of chloride ions was confirmed by gravimetric analysis with $AgNO_3$.
[29] We treated $\mathbf{7_{Cl}}$ with $NH_4PF_6$ in a metathesis reaction. See Experimental Section for reaction details.
[30] A. T. Baker, H. A. Goodwin, *Aust. J. Chem.* **1985**, *38*, 207–214.
[31] W. Ding, C. T. Sanderson, R. C. Conover, M. K. Johnson, I. J. Amster, C. Kutal, *Inorg. Chem.* **2003**, *42*, 1532–1537.
[32] J. K. Pudelski, D. A. Foucher, C. H. Honeyman, A. J. Lough, I. Manners, S. Barlow, D. O'Hare, *Organometallics* **1995**, *14*, 2470–2479.
[33] Kutal and co-workers have shown that the presence of MLCT character in the low-energy excited states of benzoyl-substituted ferrocenes enables photochemical cleavage of the iron–Cp bond, see Y. Yamaguchi, C. Kutal, *Inorg. Chem.* **1999**, *38*, 4861–4867.
[34] S. Barlow, M. J. Drewitt, T. Dijkstra, J. C. Green, C. O'Hare, D. Whittinghan, H. H. Wynn, D. P. Gates, I. Manners, J. M. Nelson, J. K. Pudelski, *Organometallics* **1998**, *17*, 2113–2120.
[35] G. Masson, P. Beyer, P. W. Cyr, A. J. Lough, I. Manners, *Macromolecules* **2006**, *39*, 3720–3730.
[36] Y. Ni, R. Rulkens, I. Manners, *J. Am. Chem. Soc.* **1996**, *118*, 4102–4114.
[37] A. B. Pangborn, M. A. Giardello, R. H. Grubbs, R. K. Rosen, F. J. Timmers, *Organometallics* **1996**, *15*, 1518–1520.
[38] Z. Otwinowski, W. Minor, *Methods Enzymol.* **1997**, *276*, 307–326.
[39] G. M. Sheldrick, SHELXTL/PC V 5.1, Bruker Analytical X-ray Systems: Madison, WI, **1997**.
[40] A. L. Spek, *J. Appl. Crystallogr.* **2003**, *36*, 7–13.
[41] W. Finckh, B.-Z. Tang, D. A. Foucher, D. B. Zamble, R. Ziembinski, A. Lough, I. Manners, *Organometallics* **1993**, *12*, 823–829.
[42] D. A. Foucher, C. H. Honeyman, A. J. Lough, I. Manners, J. M. Nelson, *Acta Crystallogr. Sect. C* **1995**, *51*, 1795–1799.

  

[43] J. M. Nelson, P. Nguyen, R. Petersen, H. Rengel, P. M. Macdonald, A. J. Lough, I. Manners, N. P. Raju, J. E. Greedan, S. Barlow, D. O'Hare, *Chem. Eur. J.* **1997**, *3*, 573–584.

[44] V. V. Dement'ev, F. Cervantes-Lee, L. Parkanyi, H. Sharma, D. O'Hare, C. Whittinham, K. H. Pannell, M. T. Nguyen, A. Diaz, *Organometallics* **1993**, *12*, 1983–1987.

Received: March 16, 2007
Published online: July 26, 2007

  